

Self-sufficient flow-biocatalysis by co-immobilization of pyridoxal 5'-phosphate and ω -transaminases onto porous carriers

Ana I. Benítez-Mateos,[†] Martina L. Contente,[§] Susana Velasco-Lozano,[‡] Francesca Paradisi,^{§}
and Fernando López-Gallego,^{‡,*}*

[†] Heterogeneous biocatalysis laboratory. CICbiomaGUNE. Paseo Miramón 182. Edificio empresarial “C”. 20014. San Sebastián (Spain).

[§] School of Chemistry, University of Nottingham, University Park. Nottingham NG7 2RD (UK).

[‡] Heterogeneous biocatalysis laboratory, Instituto de Síntesis Química y Catálisis Homogénea (ISQCH-CSIC). University of Zaragoza. C/ Pedro Cerbuna 12. 50009. Zaragoza (Spain).

^{*} ARAID, Aragon I+D foundation. Zaragoza (Spain).

KEYWORDS: ω -transaminase, enzyme immobilization, cofactor co-immobilization, self-sufficient biocatalyst, flow reactions.

ABSTRACT

We expanded the application of self-sufficient heterogeneous biocatalysts containing co-immobilized ω -transaminases and pyridoxal 5'-phosphate (PLP) to efficiently operate packed-bed reactors in continuous flow. Using a ω -transaminase from *Halomonas elongata* co-immobilized with PLP onto porous methacrylate-based carriers coated with polyethyleneimine, we operated a packed-bed reactor continuously for up to 50 column volumes at 1.45 mL x min⁻¹ in the enantioselective deamination of model amines (α -methylbenzyl amine), yielding > 90% conversion in all cycles without exogenous addition of cofactor. In this work, we expanded the concept of self-sufficient heterogeneous biocatalysts to other ω -transaminases such as the ones from *Chromobacterium violaceum* and *Pseudomonas fluorescens*. We found that enzymes with lower affinities towards PLP present lower operational stabilities in flow, even when co-immobilizing PLP. Furthermore, ω -transaminases co-immobilized with PLP were successfully implemented for the continuous synthesis of amines and the sustainable metrics were assessed. These results give some clues to exploit PLP-dependent ω -transaminases under industrially relevant continuous operations in a more cost-effective and environmentally friendly process.

INTRODUCTION

The synthesis of optically pure amines is essential to manufacture a plethora of commodities, agrochemicals and pharmaceuticals.¹ In the last decade, biocatalysis has offered efficient and environmentally sustainable solutions to incorporate amine groups into organic molecules under mild conditions and with exquisite regio and stereoselectivities.²⁻⁴ Pyridoxal 5'-phosphate (PLP)-dependent ω -transaminases (ω TAs) efficiently catalyze the asymmetric amination of ketones to yield optically pure amines with quantitative yields.^{5, 6} There are dozens of examples where different ω TAs have been engineered to aminate industrially relevant molecules.^{5, 7}

This family of enzymes transfers amino groups from sacrificing amines or amino acids to the starting ketones or aldehydes.⁶ Although the PLP is bound to ω TAs through a reversible imine bond, scaled-up biotransformations using high substrate concentrations require exogenous PLP to achieve high amine yields (50-100 mM).^{8, 9} Like other cofactor-dependent enzymes, the exogenous addition of PLP complicates the work-up because it must be separated from the final products increasing the process costs. Fortunately, catalytic amounts of PLP (0.1-2mM) are enough to accomplish the amine transfer reaction because ω TAs recycle such cofactor during their catalytic cycle. Nevertheless, the separation of both soluble cofactors and biocatalysts beside the low stability of ω TA pose important hurdles to scale-up processes.

Immobilization of ω TAs is proven an efficient approach to increase the operational stability of these biocatalysts as well as to intensify the amination process with the aim of achieving both higher productivities and yields.¹⁰ Several ω TAs have been immobilized onto a great variety of carriers and using different immobilization strategies, but unfortunately, some of the immobilized preparations resulted less efficient and stable than the soluble ones.¹⁰⁻¹³ This means that the

immobilization protocol must be carefully selected to keep catalytic efficiency and gain enzyme stability¹⁴. In the particular case of ω TAs, their immobilization is challenging because random multi-point covalent attachments through short irreversible bonds often distort their 3D structures, dramatically inactivating them. In spite of these difficulties, some immobilization protocols provided highly robust heterogeneous biocatalysts enabling process intensification of amine synthesis using packed-bed reactors (PBR).^{12, 13} Flow-biocatalysis can lead the development of more efficient chemical synthesis since it gains control over several key reactor and reaction parameters. For example, the oriented immobilization and further covalent attachment of an ω TA from *Halomonas elongata*¹⁵ onto methacrylate porous beads has been integrated into a continuous process coupled with a scavenger for the in-line synthesis and purification of different optically pure amines.¹²

Continuous operation of enzymatic transamination contributes for process intensification so far; however, those systems still require the exogenous addition of PLP that can limit their economic feasibility for the synthesis of low-added value products.^{12, 13} Ideally, PLP and enzyme should be co-reused to increase their operational life-span and thus increasing the cost efficiency of the processes. As far as we now, just one example has been reported where PLP has been incorporated into the solid phase of heterogeneous biocatalysts to operate in flow.¹⁶ Andrade et al. physically co-adsorbed PLP and whole cells harboring a ω TA onto methacrylate polymeric beads. The newly generated biocatalyst was able to synthesize optically pure α -alkoxy- and α -aryloxy isopropyl amines in flow with negligible lixiviation of PLP. However, this system must operate in organic reaction media to avoid the cofactor lixiviation.

Recently, our group has developed novel strategies to co-immobilize phosphorylated cofactors and enzymes onto a plethora of porous beads in order to fabricate self-sufficient heterogeneous

biocatalysts not requiring exogenous addition of cofactors.^{17, 18} Asymmetric reduction of ketones has been successfully accomplished using these systems in an aqueous environment. Redox cofactors (NAD(P)H) and enzymes¹⁷ remained bound to the resin under flow conditions for more than 100 hours of operation. This strategy was successful because the phosphate groups of the cofactors establish an intraporous association/dissociation equilibrium with the positively charged surface of the carriers, which allows them travelling from one active site to the other without diffusing out to the bulk.¹⁷ Under these conditions, the system is highly stable over several operational cycles without the need for exogenous cofactor.

In this work, we have exploited the co-immobilization of PLP and several ω TAs (from *Halomonas elongata*¹⁵, He- ω TA, *Chromobacterium. violaceum*¹⁹, Cv- ω TA, and *Pseudomonas fluorescens*¹⁹, Pf- ω TA) to demonstrate the self-sufficient synthesis of chiral amines. We co-immobilized ω TA and PLP onto commercial methacrylate beads functionalized with different reactive groups; cobalt-chelates, epoxides and positively charged amines (Table 1). These self-sufficient heterogeneous biocatalysts have been successfully integrated into flow PBR to perform continuous transamination reactions in buffer environment and without exogenous supply of PLP.

Table 1. Different architectures of self-sufficient heterogeneous biocatalysts based on co-immobilized ω TA and PLP.

Code	Carriers			
	Pu-Co ²⁺ /hA	Pu-Co ²⁺ /eA	EC-Co ²⁺ /eA	EC-Co ²⁺ /PEI
Commercial name	ECR8215F	ECR8215F	EC-EP/S	EC-EP/S
Particle size	150-300 μ m	150-300 μ m	100-300 μ m	100-300 μ m
Pore size	120-180 nm	120-180 nm	10-20 nm	10-20 nm
Aminated molecule	Hydroxylamine	Ethanolamine	Ethanolamine	Polyethyleneimine
Scheme				

Purolite ECR8215F (Pu-Co²⁺) and Sepabeads EC-EP/S (EC-Co²⁺) carriers were activated with different aminated molecules; hydroxylamine (/hA), ethanolamine (/eA) and 60 kDa polyethyleneimine (/PEI). Black dashed lines show the coordination bonds between His(6x)-tag of the protein and cobalt chelates displayed at the carrier surface.

EXPERIMENTAL SECTION

Reagents

Lifetech Purolite ECR 8215F and Sepabeads EC-EP/S were kindly donated by Purolite Ltd. (Llantrisant, U.K.) and Resindion S.R.L., respectively. Polyethyleneimine 60 kDa 50 % wt aq. solution, branched was purchased from ACROS OrganicsTM. Ethanolamine, Hydroxylamine, (S)-phenylethylamine, rhodamine B isothiocyanate, iminodiacetic acid, cobalt (II) chloride, trans-cinnamaldehyde, *p*-nitrobenzaldehyde, sodium pyruvate, *S*-(α)-Methylbenzylamine and PLP were acquired from Sigma-Aldrich (St. Louis, IL). UV transparent 96-well plates and 1 mL cuvettes were purchased from Thermo Fisher Scientific. μ -Slides with 8 wells were purchased from ibidi (Planegg, Germany). All other salts and reagents were of analytical grade.

Activation of carriers

Purolite. Epoxy-purolite beads were incubated with 0.5 M iminodiacetic acid (IDA) at pH 11.0 for 3 hours at room temperature and orbital shaking. Samples were intensively washed with distilled H₂O. A solution of 30 mg x mL⁻¹ CoCl₂ was added (1:10 w/v) and incubated for 1 hour. After a washing step, Pu-Co²⁺/eA was prepared adding 0.5 M ethanolamine at pH 11.0 and incubated overnight under orbital shaking. In case of Pu-Co²⁺/hA, 0.5 M hydroxylamine at pH 11.0 was added and incubated overnight under orbital shaking.

Sepabeads. Epoxy-sepabeads were firstly activated with cobalt as previously described.²⁰² EC-Co²⁺/eA was prepared by adding 0.5 M ethanolamine at pH 11.0 and incubating overnight under orbital shaking. For preparation of EC-Co²⁺/PEI, a solution of 5 mg x mL⁻¹ PEI in 100 mM sodium bicarbonate buffer at pH 10.0 was added after protein immobilization and incubated for 1 hour under orbital shaking.

Expression and purification of enzymes

He- ω TA and Cv- ω TA were expressed and purified following a previously reported protocol.¹⁴ For the expression of Pf- ω TA, 1 mL of an overnight culture of *E. coli* BL21 (previously transformed with the plasmid pET28b_Pf- ω TA) was inoculated in a 50 mL of LB medium, containing kanamycin at final concentration of 30 μ g x mL⁻¹. The resulting culture was incubated at 37°C with energetic shaking until the OD_{600nm} reached 0.4-0.6. At that point, the culture was induced with 0.01 mM 1-thio- β -d-galactorpyranoside (IPTG). Cells were grown at 21°C for 16 hours and then harvested by centrifugation at 4211 g for 30 min at 4°C. The resulting pellet was resuspended in 5 mL of 10 mM sodium phosphate buffer at pH 7.3 containing 0.1 mM PLP. Cells were sonicated (Sonic Vibracell VCX750) at amplitude= 20 %, cycles= 5 sec ON, 5 sec OFF, for 30

min. The suspension was centrifuged at 10528 *g*, 30 min, 4°C. The supernatant containing the enzyme was collected and stored at 4°C. Protein concentration was determined by analysis of SDS-PAGE gel bands (with a standard curve of BSA) using the software ImageJ. The purification process of He- ω TA, Cv- ω TA and Pf- ω TA was followed by SDS-PAGE (Figure S1).

Protein quantification

Protein was quantified by Bradford's method²¹ adapted to 96-well plates. Briefly, 5 μ L of enzyme solution were mixed with 200 μ L of Bradford reagent, incubated at room temperature for 5 min. Then the absorbance was measured at 595 nm and the protein content was estimated employing a calibration curve using BSA as a standard.

Enzyme immobilization

10 mL of enzyme solution (0.1 – 0.5 mg x mL⁻¹) containing 0.1 mM of PLP in 50 mM sodium phosphate buffer at pH 8, were added to 1 g of carrier and incubated under orbital shaking for 4 hours (He- ω TA and Cv- ω TA), and for 1 hour (Pf- ω TA) at room temperature. Then, the suspension was filtered and washed 3 times with 10 volumes of phosphate buffer.

Cofactor immobilization

Immobilization of PLP was achieved as described by Velasco-Lozano et al.¹⁶ Briefly, 10 volumes of 1 mM cofactor in 10 mM sodium phosphate buffer at pH 7.3 were incubated with 1 g of methacrylate beads with previously immobilized enzymes. The suspension was kept under orbital shaking for 1 h at room temperature. The sample was then filtered and washed three times with 10 mM sodium phosphate buffer at pH 7.3. The immobilized PLP was determined by measuring the

absorbance at 390 nm of 100 μ L of the flow-through in a 96-well microplate using a Varian Cary 50 scan UV-visible spectrophotometer. The PLP immobilization yield was calculated as follows;

$$\Psi (\%) = 100 - ([\text{PLP}]_{\text{supernatant}} / [\text{PLP}]_{\text{offered}}) \times 100$$

[PLP]_{supernatant} means the PLP concentration in the supernatant after being incubated with the carrier and [PLP]_{offered} means the PLP concentration in the supernatant before being incubated with the carrier. PLP concentration was determined spectrophotometrically.

Enzyme kinetics

The activity of immobilized ω -transaminases was determined by mixing 50 mg of biocatalyst and 10 mL of reaction mixture (2.5 mM pyruvate, 2.5 mM *S*-(α)-methylbenzylamine and 0.25 % DMSO in 10 mM phosphate buffer pH 7.3) into a 15 mL reaction tube cap. The final reaction mixture was incubated at room temperature under orbital shaking. The absorbance at 245 nm was measured along the time as single readings using Brand UV-cuvettes in a Varian Cary 50 scan UV-visible spectrophotometer. One unit of ω -transaminase activity was defined as the amount of enzyme required for the production of 1 μ mol of acetophenone per minute.

Fluorescence techniques

Rhodamine-labeling of He- ω TA. An enzyme solution was mixed (1:1 molar ratio) with rhodamine B (from a stock solution, 1 mg \times mL⁻¹ in DMSO) in 100 mM sodium phosphate at pH 8.0 and incubated for 1 h with gentle agitation at 25 $^{\circ}$ C in darkness. This step allows the acylation reaction between the primary amines from proteins and the isothiocyanates from rhodamine B to

form a thiourea.²² Later, the unreacted rhodamine B was removed by filtration of the labeling mix through a tangential ultrafiltration unit (10 kDa) washing with 25 mM sodium phosphate buffered solution at pH 7 until the flow-through solution was colourless.

CLSM (Confocal laser scanning microscopy) imaging. Enzyme localization was observed using a ZEISS confocal microscope 510 with an excitation laser (λ : 514 nm) and the emission filter LP505. Since PLP exhibits autofluorescence, the spatial distribution of PLP across the EC-Co²⁺/PEI beads was determined using CLSM with an UV excitation laser (405 nm) and the emission filter LP420. Images were processed with the software ZEN2012.

Spatial distribution study. The labeled enzyme was further immobilized at 1 mg x g⁻¹ onto EC-Co²⁺ beads. After PEI coating, PLP was co-immobilized at 7.5 $\mu\text{mol x g}^{-1}$. The beads suspension was filtered and placed on a microscope slide. In order to improve the match in refractive index between the medium and the opaque beads, a drop of glycerol was placed onto the beads.

PLP immobilization kinetics. 20 mg of EC-Co²⁺/PEI were incubated with 200 μL of 1mM PLP solution containing 50% glycerol in sodium phosphate buffer pH 7.3 in a 8-well μ -slide. PLP autofluorescence was monitored along the time.

Desorption experiments. Three desorptions of PLP were carried out. 50 mg of EC-Co²⁺/PEI with immobilized PLP were incubated with 500 μL of 4 M NaCl, 1 M Ethanolamine or a mixed solution with 4 M NaCl and 1 M Ethanolamine. The suspensions were incubated at room temperature for 1 hour. After filtration, three washing steps with phosphate buffer were performed. The beads were observed by adding a drop of glycerol. Finally, PLP was immobilized for second time by adding 400 μL of 1 mM PLP solution to 40 mg of EC-Co²⁺/PEI (previously treated with ethanolamine).

Flow deamination reactions

The continuous flow biotransformations were performed using a R2+/R4 flow reactor commercially available from Vapourtec equipped with an Omnifit glass column (6.6 mm i.d x 100 mm length) filled with 1.0 g of biocatalyst. An amino acceptor substrate solution (20 mM pyruvate in phosphate buffer) and an amino donor solution (50 mM *S*-(α)-methylbenzylamine and 5% DMSO in phosphate buffer) were prepared. After mixing with a T-tube the resulting concentrations were 10 mM for the amino acceptor and 25 mM for the amino donor. 50 mM phosphate buffer at pH 8.0 was used for flow-reactions with added PLP (0.1 mM) and when exogenous PLP was not added. 10 mM phosphate buffer at pH 7.3 was used for flow-reactions when PLP was co-immobilized. The resulting flow stream was driven to the column packed bed reactor with the biocatalyst (packed bed reactor volume: 1.3 - 1.45 mL). A first washing step with a flow rate of 0.4 mL x min⁻¹ was performed for 30 minutes. Then, the flow rate was varied in order to obtain the desired residence time. The resulting flow product was analysed by HPLC following a previously reported protocol.²⁰

Flow synthesis of amines

The continuous flow synthesis of cinnamylamine and *p*-nitrobenzylamine were performed using the equipment described above. The synthesis of cinnamylamine, was performed preparing solution of 20 mM *trans*-cinnamaldehyde and 10% DMSO in phosphate buffer and mixing it with 1 M L-alanine in phosphate buffer. After the mixing, the concentrations of *trans*-cinnamaldehyde and L-alanine were 10 mM and 500 mM, respectively. In the synthesis of *p*-nitrobenzylamine, the amino acceptor solution (10 mM *p*-nitrobenzaldehyde and 20 % DMSO in phosphate buffer) was mixed with the amino donor solution (1 M L-alanine in phosphate buffer). After the mixing, the concentrations of *p*-nitrobenzaldehyde and L-alanine were 5 mM and 500 mM, respectively. The resulting flow product was analysed by HPLC following a previously reported protocol.²⁰

RESULTS AND DISCUSSION

To expand the concept of self-sufficient heterogeneous biocatalysts to amine biotransformations using PLP-dependent ω TAs, commercial porous methacrylate beads activated with epoxide groups were functionalized with cobalt-chelates and then blocked with either hydroxylamine or ethanolamine (Figure 1), giving rise to carriers named as Pu-Co²⁺/hA and Pu-Co²⁺/eA, respectively (Table 1). Firstly, we optimized the PLP immobilization conditions to avoid its lixiviation in reaction. To this aim, we firstly co-immobilized He- ω TA and PLP onto Pu-Co²⁺/eA under different buffered conditions. We must point out that both enzyme and cofactor were reversibly bound to this carrier through coordination and ionic bonds, respectively. Low ionic strength (10 mM) phosphate buffer and Tris-HCl buffer at pH 7.3 were the most effective conditions to minimize both PLP and enzyme lixiviation after 3 consecutive washes (Figure S2). The use of phosphate instead Tris-HCl buffer is indeed beneficial for the process, since phosphate promotes the stability of the apoenzyme and prevents its irreversible unfolding.²³ For these reasons, phosphate buffer was selected to carry out the enzymatic reactions. The deamination activity of immobilized He- ω TA towards *S*- α -methylbenzyl amine (*S*-MBA) was significantly lower when PLP was adsorbed onto Pu-Co²⁺/hA than when it was onto Pu-Co²⁺/eA (Figure S3), indicating that the cofactor was catalytically more available when the solid surface was activated with ethanolamine.

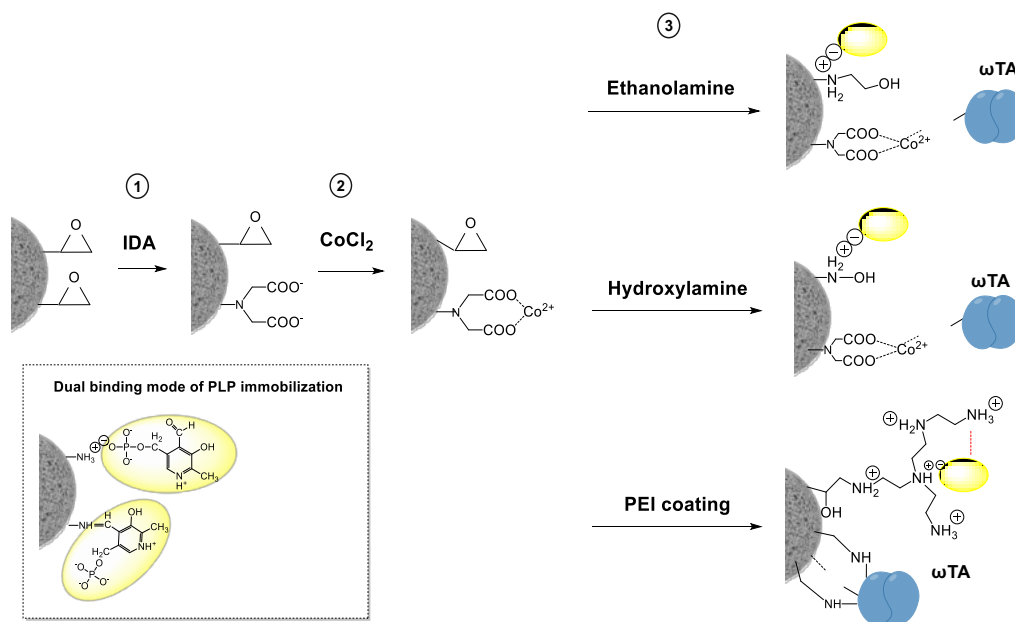


Figure 1. Preparation of self-sufficient biocatalysts. Methacrylate-based carriers activated with epoxy groups were functionalized with iminodiacetic acid (IDA) (1) and then with cobalt chloride (2) resulting in cobalt chelates that drive the His-tagged ω -transaminase immobilization (black dashed line). Then, the carrier was also activated with amine groups from ethanolamine, hydroxylamine and polyethyleneimine for the PLP co-immobilization (3). Red asterisk highlights the dual binding of PLP on PEI layer (left bottom inlet).

Finally, we tested the effect of the carrier architecture on PLP binding by using methacrylate carriers activated with ethanolamine at two different pore sizes (Table 1). Methacrylate beads (EC-Co²⁺/eA) with smaller pores (size = 10-20 nm) loaded up to 8.6 $\mu\text{mol}_{\text{PLP}} \times \text{g}_{\text{carrier}}^{-1}$ and only 10% of the bound cofactor was lixiviated after three washes. On the contrary, Pu-Co²⁺/eA with larger pores (size = 120-180 nm) loaded 3 times less PLP (2.8 $\mu\text{mol}_{\text{PLP}} \times \text{g}_{\text{carrier}}^{-1}$) than EC-Co²⁺/eA and underwent 43% lixiviation of the bound cofactor after three washing steps (Figure S4). Although the carriers were loaded with different amounts of PLP, co-immobilized He- ω TA

expressed similar deamination rate and ketone yield without adding exogenous cofactor after the first batch cycle (Figure S5) and after the first column volume in flow (Figure 2). However, EC-Co²⁺/eA biocatalyst presented a slightly longer operational half-life time (133 minutes) in flow than the Pu-Co²⁺/eA one (115 minutes). Nevertheless, the activation of methacrylate beads with ethanolamine and cobalt chelates (EC-Co²⁺/eA) was not enough to operate the self-sufficient heterogeneous biocatalysts for longer times with high yields (Figure 2). PLP was observed in the flow-through after 20 minutes, suggesting that its lixiviation might be one of the main causes for the biocatalyst inactivation. Furthermore, the enzyme was immobilized through reversible metal coordination bonds between the His(6x)-tag fused at the protein N-terminus and the cobalt-chelates groups displayed in the carrier surface (Figure 1).

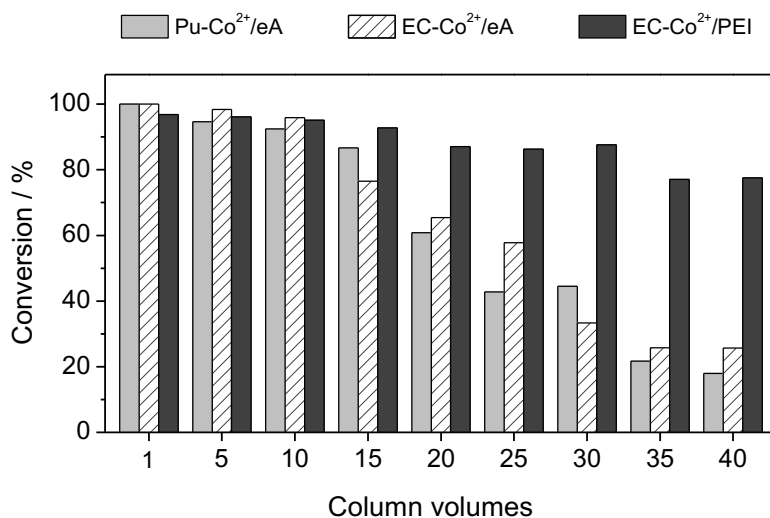


Figure 2. Stability test of different self-sufficient biocatalysts operating in flow at 0.3 mL x min⁻¹. He- ω TA was immobilized at 1 mg x g⁻¹ onto three different carriers; Pu-Co²⁺/eA, EC-Co²⁺/eA and EC-Co²⁺/PEI, that loaded 1.7, 7.8 and 7.5 $\mu\text{mol}_{\text{PLP}} \times \text{g}_{\text{carrier}}^{-1}$, respectively. Each column volume corresponds to 5 minutes.

This common strategy for protein purification has been recently and successfully exploited for a subsequent ten-minute protein purification and operation under continuous-flow conditions to yield *p*-nitrophenol using a bi-enzyme (alkaline phosphatase and phosphodiesterase) immobilized system.²⁴ However, in our set-up, the reversible immobilization of He- ω TA failed since the enzyme was partially release, leading the yield decay observed in Figure 2.

To avoid both enzyme and cofactor lixiviation, and consequently improve the performance of the biocatalyst, we modified its architecture design to establish irreversible bonds between the enzyme and the solid surface and optimize the reversible interactions between PLP and the surface matrix. After site-directly immobilization of He- ω TA through the His(6x)-tag, the remaining epoxide groups were exploited to irreversibly attach the oriented enzyme and allow the PEI coating upon the immobilization (EC-Co²⁺/PEI). As result, the enzyme was oriented and irreversibly immobilized through a multivalent attachment, while PLP established an association/dissociation equilibrium with the PEI layer, through both ionic bridges and reversible imine bonds (Schiff's bases) (Figure 1, Table 1). Such dual interaction was supported by desorption experiments that demonstrate quantitative PLP elution from EC-Co²⁺/PEI requires both high ionic strength and ethanolamine concentrations to break ionic bonds and Schiff's bases, respectively (Figure 3A). Unlike other phosphorylated cofactor such as NAD(P)H, aldehyde groups and phosphate groups from PLP can establish that dual interaction with the primary amines and the positively charged amine groups of PEI, respectively. The reversible imines bonds between PLP and PEI mimic the chemistry that anchors such cofactor into the ω TA active site. Moreover, once PLP is fully eluted, the carrier can be equilibrated and re-charged with fresh PLP (Figure 3A, right side panel). Finally, this architecture significantly increased the operational life of the self-sufficient heterogeneous

biocatalysts in continuous deamination reactions, since the reaction conversion decayed less than 20% after 200 minutes of operation (40 column volumes) (Figure 2).

The higher capacity of EC-Co²⁺/PEI to reversibly bound PLP through a dual binding is supported by its $K_d = 20.4 \pm 0.9 \mu\text{mol} \times \text{g}^{-1}$, which is significantly lower than K_d values determined for EC-Co²⁺/eA ($K_d = 27.4 \pm 1.2 \mu\text{mol} \times \text{g}^{-1}$) and Pu-Co²⁺/hA ($K_d = 121.4 \pm 5.8 \mu\text{mol} \times \text{g}^{-1}$) carriers. These equilibrium constants were determined by fitting experimental data to Langmuir isotherm equation (Figure S6). The PLP adsorbed in EC-Co²⁺/PEI falls in the same order of magnitude that the PLP equilibrium constants determined with similar positively charged surfaces.¹⁷ Hence, the nature of the interaction between PLP and carrier surface dictates how strong PLP is bound to the matrix. Therefore, PEI containing primary, secondary and tertiary amines capable to establish two type of interactions with PLP; salt bridges and imine bonds retains more efficiently the cofactor than surfaces only activated with secondary amines (EC-Co²⁺/HA and EA) that limit PLP adsorption to ionic interactions.

Additionally, confocal microscopy of EC-Co²⁺/PEI particles co-immobilizing PLP and He- ω TA revealed that both molecules co-localized within the same particle but with different spatial distributions (Figure 3B). While He- ω TA is located at the outer surface of the porous beads, PLP is homogeneously distributed across the whole carrier surface. The spatial organization of both PLP and enzyme remained stable even after one-week storage at 4° C, demonstrating that the enzyme cannot migrate inside the porous surface because it is irreversibly bound, while the cofactor is unable to diffuse out of the beads (Figure 3B). PLP binding monitored by time-lapse fluorescence microscopy demonstrates the reversible nature of PLP interaction since cofactor molecules are primarily adsorbed to the outer surface of the beads (short times), to further migrate across the

carrier porous structure (Figure 3C). The cofactor migration proves that PLP molecules can reach enzyme active sites within the carrier microstructure but without diffusing out to the reaction bulk.

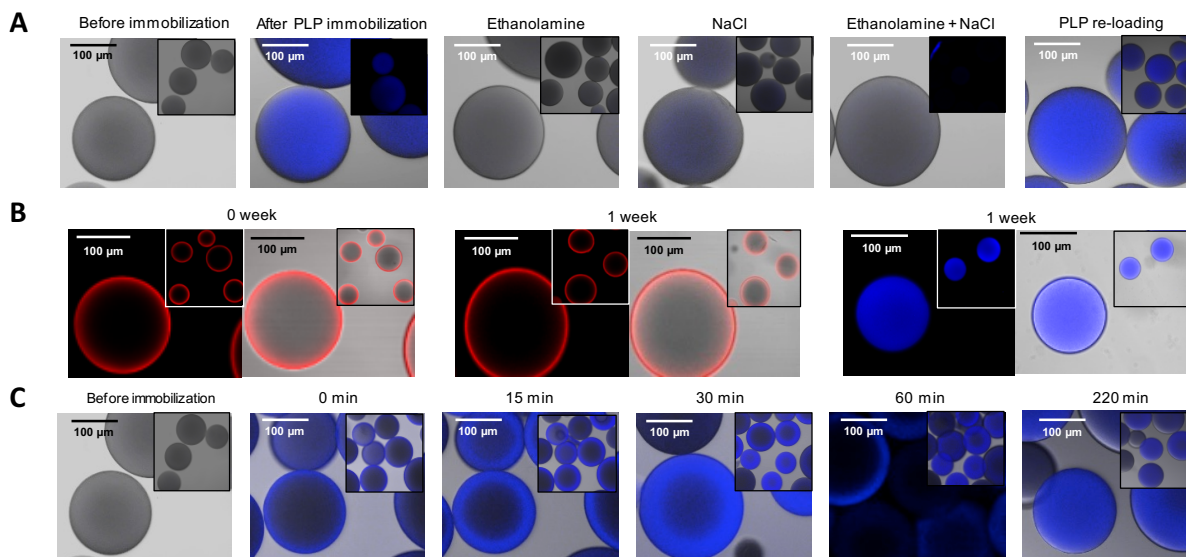


Figure 3. Single-particle studies by CLSM imaging. A) From left to right, porous beads (EC-Co²⁺/PEI) *n* before and after incubation with PLP (blue). The porous beads immobilizing PLP incubated with 1 M ethanolamine, 2 M NaCl and both 1 M ethanolamine and 2 M NaCl. Finally, PLP was again re-loaded on EC-Co²⁺/PEI after washing steps. Images show the overlay of fluorescence and brightfield signals. B) Spatial distribution of rhodamine-labeled He-ωTA (red) and PLP (blue) within the self-sufficient biocatalyst. Images were taken when the biocatalyst was prepared (0 week) and after storage at 4 °C for a week. The left side image of each panel shows the fluorescence signal and the right one merges the fluorescence and the brightfield signals. C) PLP immobilization kinetics along the time. Images show the overlay of fluorescence and brightfield signals.

Functional data together with microscopic analysis indicate that the nature and the density of positively charged groups as well as the pore size of the methacrylate beads are determinant

parameters to allow the PLP shuttling between the enzyme active sites without leaving the pore microenvironment.

Flow rate is one of the most important parameters that govern productivity of continuous operations. Once both PLP and He- ω TA were optimally co-immobilized onto EC-Co²⁺/PEI, this self-sufficient heterogeneous biocatalyst was tested at two different flow rates; 0.3 and 1.45 mL x min⁻¹ (Figure 4). Operating the PBR at higher flows, the specific productivity of He- ω TA increased from 6.79 to 33.95 $\mu\text{mol}_{\text{product}} \times \text{min}^{-1} \times \text{mg}_{\text{enzyme}}^{-1}$ and remained constant after processing 70 mL of reaction mixture (50 column volumes). This result clearly indicates that bound PLP is not lixiviated even under high flow rates, strongly favoring enzymatic productivity.

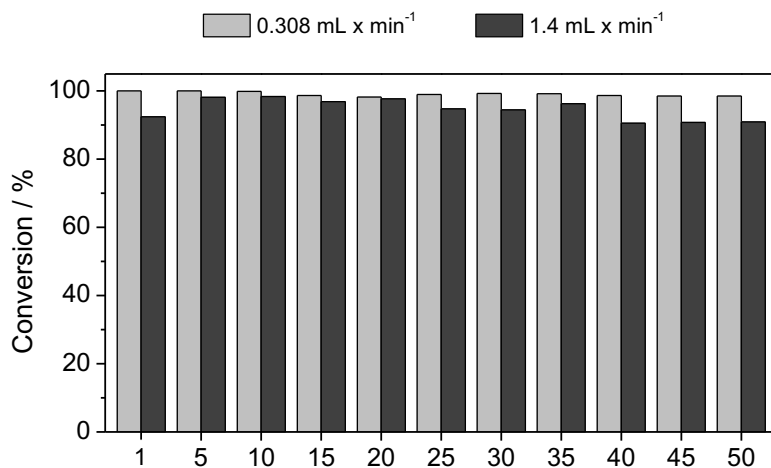


Figure 4. In flow stability test of the self-sufficient biocatalyst with co-immobilized He- ω TA (5 mg x g⁻¹) and PLP (7.8 $\mu\text{mol} \times \text{g}^{-1}$) onto EC-Co²⁺/PEI along the time. For the flow rate at 0.308 mL x min⁻¹, each column volume corresponds to 5 minutes and for the flow rate at 1.45 mL x min⁻¹, each column volume took 1 minute.

Therefore, this PBR successfully operated at $1.45 \text{ mL} \times \text{min}^{-1}$, the highest flow rate ever reported using co-immobilized enzyme and cofactor¹⁶⁻¹⁸ and one of the highest ($0.1\text{-}1.7 \text{ mL} \times \text{min}^{-1}$) using immobilized enzymes supplied with exogenous cofactor.^{11-13, 25}

In principle, this promising approach may be expanded to other ω TAs in order to fabricate a battery of self-sufficient heterogeneous biocatalysts with different catalytic properties (stability, selectivity, kinetics). Based on the same architecture, two additional N-terminus His-tagged ω TAs (Cv- ω TA and Pf- ω TA) were immobilized onto EC-Co²⁺ and further coated with PEI to finally absorb PLP as described above. In all cases, > 90 % of offered activity ($5 \text{ mg}_{\text{enzyme}} \times \text{g}_{\text{carrier}}^{-1}$) was immobilized and each heterogeneous biocatalyst loaded $7\text{-}7.5 \text{ } \mu\text{mol}_{\text{PLP}} \times \text{g}_{\text{carrier}}^{-1}$ (Table 2). As shown in Figure 1, the enzymes were oriented and irreversibly immobilized through a multi-valent attachment, while cofactor establishes an association/dissociation equilibrium with the PEI layer based on a dual interaction mode. Upon the immobilization process, the three ω TAs recovered 8-11% of their specific activity in solution (Table 2). The low recovered activities might be caused by mass transport restrictions underlying the measurement set up. Enzyme activities were determined by spectrophotometric analysis using plate readers whose orbital shaking is not optimized to measure highly dense carriers with large particle size such as the porous methacrylate beads utilized in this work. In this context, the substrate likely suffers important diffusion barriers for being transported from the reaction bulk to the porous surface of the carrier, where both enzyme and cofactor are located. In fact, when enzyme activity was measured under more vigorous shaking, the expressed activity of ω TA upon immobilization was increased up to 90% (Table S1). Noteworthy, the three ω TAs herein studied showed similar specific activity towards soluble and immobilized PLP, which demonstrates that the cofactor is fully available and can access to the ω TA active sites (Table 2).

Table 2. Immobilization yields and specific activities of immobilized ω -transaminases onto EC- Co^{2+} /PEI.

Enzyme	Immobilization yield (%)	Protein load ($\text{mg}_{\text{enzyme}} \times \text{g}_{\text{carrier}}^{-1}$)	Cofactor load ($\mu\text{mol}_{\text{PLP}} \times \text{g}_{\text{carrier}}^{-1}$)	Immobilized specific activity ($\text{U} \times \text{mg}^{-1}$) and [Relative recovered activity (%)]	
				Free PLP	Co-immobilized PLP
He- ω TA	99 \pm 1.81	4.95	7.5 \pm 0.08	0.29 \pm 0.02 [11]	0.27 \pm 0.02 [10]
Cv- ω TA	92 \pm 3.42	4.62	7.4 \pm 0.15	0.13 \pm 0.03 [7]	0.11 \pm 0.00 [6]
Pf- ω TA	100 \pm 0.90	5	7 \pm 0.21	0.16 \pm 0.00 [8]	0.14 \pm 0.01 [7]

Protein load of He- ω TA and Cv- ω TA was determined by Bradford assay. SDS-PAGE analysis by using ImageJ was carried out to determine the Pf- ω TA load. The enzymatic activities were measured in 96-well plates by monitoring absorbance at 245 nm. Briefly, 200 μL of a reaction mixture (2.5 mM pyruvate, 2.5 mM *S*-(α)-methylbenzylamine, 0.25% DMSO and 37.5 μM PLP in 10 mM sodium phosphate buffer at pH 7.3) were incubated with 10 μL of enzymatic solution or suspension (1:10 w/v). Immobilization yield is defined as percentage of protein that disappears from the supernatant after the immobilization. Relative recovered activity is defined as; (specific activity of immobilized enzyme/specific activity of soluble enzyme) \times 100. Specific activity was measured as above described.

Encouraged by the excellent enzymatic activity towards the immobilized cofactor, we tested the three different self-sufficient heterogeneous biocatalysts in the continuous deamination of *S*-MBA at 1.45 $\text{mL} \times \text{min}^{-1}$ (Figure 5). Interestingly, the operational performance of each biocatalyst relied on which ω TA was immobilized onto. He- ω TA maintained maximum conversion during the whole operational test producing 70 mL of 25 mM product after 50 column volumes. On the contrary, when the reactor was packed with Cv- ω TA co-immobilized with PLP, we observed a linear decay of conversion down to 30% after 50 column volumes (Figure 5). Under the same conditions, Pf- ω TA performed notably better than Cv- ω TA but slightly worse than He- ω TA. Differences on deamination efficiencies may rely on the affinity of each enzyme towards PLP. In fact, when flow reactions were performed using the different immobilized ω TAs with natural bound PLP (not exogenously added), we observed a similar trend: He- ω TA preserved the highest conversion whereas Cv- ω TA showed the lowest one after 50 cycles (Figure S7). These results suggest that high flows can detach more easily the natively bound PLP from Cv- ω TA than from He- ω TA. The unsatisfactory performance of Cv- ω TA can be explained by the low affinity of this

enzyme towards PLP ($K_d = 78 \mu\text{M}$)²³ compared to other ω TAs ($K_d = 0.25\text{-}10 \mu\text{M}$).²⁶ Hence, the operational stabilities shown in Figure 5 and S7, suggest that Pf- ω TA binds PLP better than Cv- ω TA but worse than He- ω TA.

The results shown in Figure 5 motivated us to understand whether the enzyme is stabilized by the immobilization itself, by the high effective PLP concentration in the enzyme vicinity or by a synergy of both effects. To answer that question, Pf- ω TA was immobilized with and without PLP on porous carriers functionalized with PEI, and the resulting preparations were thermally inactivated (Figure 6).

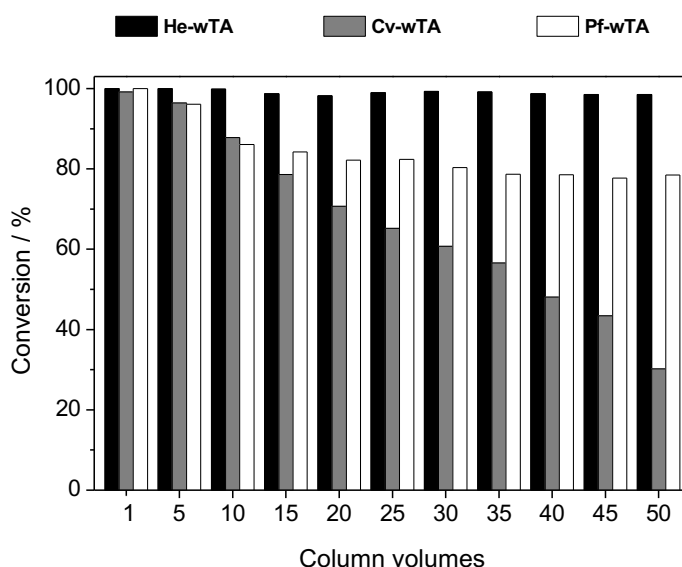


Figure 5. Continuous flow deamination reactions using different self-sufficient biocatalysts with co-immobilized ω -transaminases and PLP. He- ω TA, Cv- ω TA and Pf- ω TA were immobilized onto EC- Co^{2+} /PEI at $5 \text{ mg} \times \text{g}^{-1}$. The flow reactions were performed at $1.45 \text{ mL} \times \text{min}^{-1}$. Each column volume corresponds to 1 minute.

Likewise, soluble enzyme was inactivated either in presence or absence of PLP. Soluble Pf- ω TA suffered a dramatic inactivation in absence of PLP, as well as the enzyme immobilized without the

cofactor. Conversely, the co-immobilization of Pf- ω TA and PLP significantly stabilizes the enzyme against high temperatures.

Figure 6 shows that PLP drives to more significant thermal stabilization than protein immobilization itself. In fact, we observed a trend between the concentration of immobilized PLP and the enzyme thermal stability. When ω TA was surrounded by the highest PLP intraparticle concentration tested herein, the enzyme thermal stability was 10 times higher (Figure 6). This result indicates that the available concentration of PLP for ω TA relies on the concentration of bound PLP. Hence, enzymes surrounded by more molecules of PLP are more stable, because this cofactor stabilizes protein quaternary structure avoiding subunit dissociation.²⁰ When soluble PLP was incubated with soluble Pf- ω TA, we observed a similar stabilization effect in agreement with the data published elsewhere for Cv- ω TA.²² These experimental evidences point out that immobilization itself is not significantly stabilizing the enzyme, while the presence of PLP (both in soluble and co-immobilized forms) enormously enhances the enzyme stability.

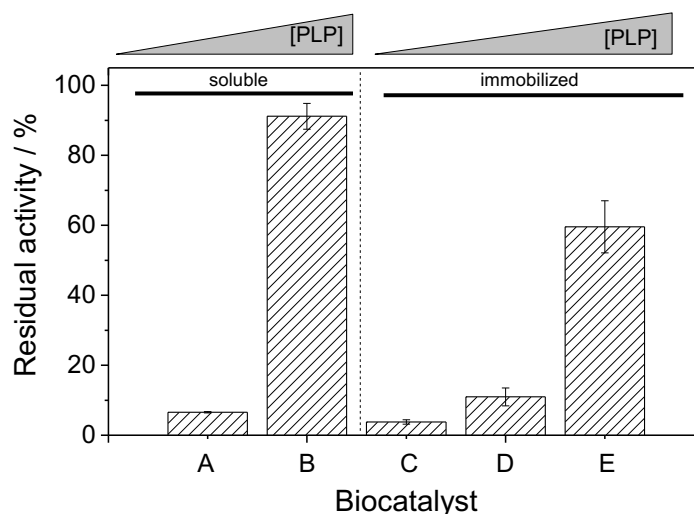
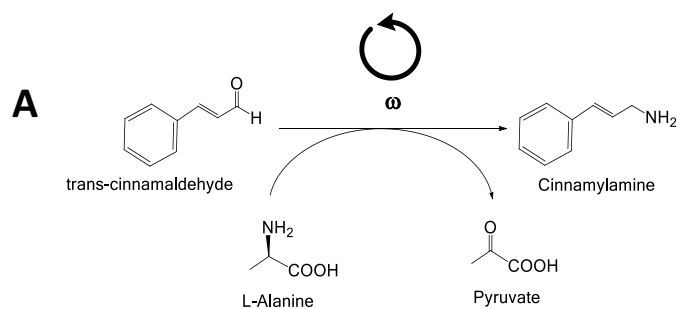


Figure 6. Stability of Pf- ω TA at different PLP concentrations. Bars represent the residual activity of the biocatalysts after 30 min of incubation at 65°C: A) Soluble Pf- ω TA. B) Soluble Pf- ω TA at 0.1 mM PLP. C) Immobilized Pf- ω TA on EC-Co²⁺/PEI. D) Co-immobilized Pf- ω TA and PLP on EC-Co²⁺/PEI at 1 $\mu\text{mol}_{\text{PLP}} \times \text{g}_{\text{carrier}}^{-1}$ and E) Co-immobilized Pf- ω TA and PLP on EC-Co²⁺/PEI at 10 $\mu\text{mol}_{\text{PLP}} \times \text{g}_{\text{carrier}}^{-1}$.

Finally, to expand the applications of this autonomous system, we performed the continuous synthesis of amines without exogenous supply of PLP (Figure 7A). A column packed with He- ω TA and co-immobilized PLP onto EC-Co²⁺/PEI, was fed with cinnamaldehyde to continuously synthesize cinnamylamine. Figure 7B shows as the self-sufficient heterogeneous biocatalyst is operationally slightly more stable than the system supplied with exogenous PLP. A similar trend was found for the synthesis of *p*-nitrobenzylamine (Figure S8).



B

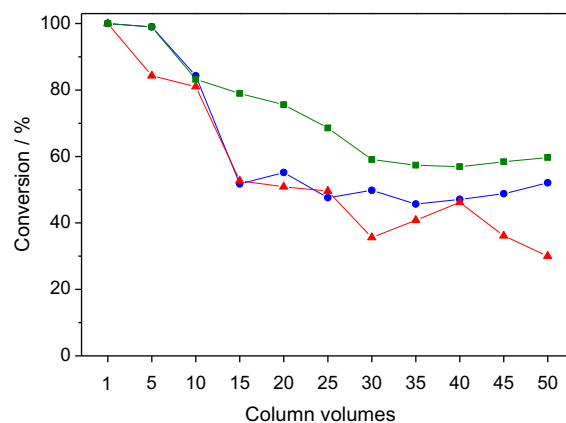


Figure 7. Synthesis of Cinnamylamine. A) Reaction scheme. B) Continuous synthesis of cinnamylamine without PLP (red triangles), with exogenous PLP (blue circles) and immobilized PLP (green squares). He- ω TA was immobilized onto EC-Co²⁺PEI at 5 mg x g⁻¹. The flow reactions were performed at flow-rate 0.725 mL x min⁻¹. Each column volume corresponds to 2 minutes.

The amine synthesis required double residence times than the deamination reaction to achieve complete conversion. In addition, the operational stability under amination conditions was significantly lower than under deamination conditions, likely due to the high concentration of L-Ala that may elute some of the bound PLP, since such needed amine donor contains amine and carboxylic groups that can compete with the dual interaction mode of PLP; imine and ionic bonds,

respectively. Hence, the alanine may provoke the cofactor lixiviation which may explain the lower yields in the amination reaction than in the deamination one.

Encouraged by the excellent results obtained for the continuous synthesis of cynamylamine, we assessed some sustainable metrics for the amination reaction shown in Figure 7 (Table S2). Considering exogenously added PLP as a reactant, the atom economy is 27% compared with the 60% obtained with the reaction catalyzed by the self-sufficient biocatalyst that incorporates both enzyme and cofactor into the solid phase. More interestingly, we determined the total E-factor and the contribution of each reactant (waste) to that total value after 50 continuous reaction cycles (Figure 7). Table 3 shows that E-factors including solvents (DMSO and water) are two orders or magnitude higher than those ones calculated ignoring them. Pleasantly, the use of immobilized PLP reduces E-factor value 1.23 times compared to the system supplied with exogenous cofactor. This reduction is mainly due to higher yields after the 50 operational cycles, but surprisingly the contribution of the soluble PLP was negligible.

Table 3. E-factor values for the continuous synthesis of cynamylamine using immobilized ω -TAs under different conditions.

PLP form	Including Solvents	E-factor contribution of each reagent ^[b] (relative contribution, %) ^[c]							Total E-factor ^[a]
		Aldehyde	Alanine	Pyruvate	PLP	DMSO	Water	Biocat	
I	YES	0,38 (0)	46 (1)	0,66 (0)	0 (0)	10 (0)	6438 (99)	15 (0)	6510
	NO	0,38 (1)	46 (74)	0,66 (1)	0 (0)	n.a	n.a	15 (24)	61
S	YES	0,67 (0)	55 (1)	0,66 (0)	0,03 (0)	13 (0)	7784 (99)	18 (0)	7871
	NO	0,67 (1)	55 (74)	0,66 (0)	0,03 (0)	n.a	n.a	18 (24)	75

[a]Total E-factor was calculated as mg of reactants / mg of cynamylamine. [b]E-factor contribution was calculated as mg of each reactant / mg of cynamylamine. [c] E-factor relative contribution of each reactant was calculated as (E-factor contribution of each reactant / Total E-factor) x 100. PLP forms; (I) immobilized; (S) soluble exogenously added.

The major contribution to the E-factor is water (99%), a reactant that is essential for the most of enzyme reactions but rarely accounted when measuring sustainability of biocatalytic processes.

Water should be considered as a waste at least that such residual water is fed back to the system or downstream purification steps are included in the process. The latter case has been shown successful in flow-biocatalysis, although sustainable metrics were not assessed¹². In the other hand, when solvents were ignored, biocatalyst contribution to the total E-factor is significant (15-18%); the second highest after the amine donor (alanine). These sustainable metrics thus suggest that both solvents and biocatalysts must be integrated in the equation that defines process sustainability. Hence, solvents and biocatalysts should be considered when assessing sustainable metrics, at least both ones can be extensively recycled.

CONCLUSIONS

In summary, we have expanded the fabrication of self-sufficient heterogeneous biocatalysts for deamination and amination reactions avoiding the exogenous supply of cofactors. To this aim, we have co-immobilized ω TAs from different origins and PLP within the same porous methacrylate beads. Within these solid materials, His-tagged ω TA is irreversibly and multivalently attached to the carrier surface, whereas PLP is bound on a polymeric bed through reversible interactions (ionic bridges and imine bonds). As result, we operated PBRs using ω TAs from different sources with different operational stability results. We suggest that such stability relies on the affinity of each immobilized enzyme towards PLP. Finally, we exploited these self-sufficient heterogeneous biocatalysts in the continuous amination of aldehydes, obtaining high amine yields along the column volumes. In addition, we assessed the sustainability metrics for this latter reaction, reflecting that water and biocatalysts (more importantly when it is immobilized) must be considered in the calculation, otherwise we dramatically underestimate E-factor values. This work advances in the development of self-sufficient biocatalytic systems that ultimately eliminate the requirement of exogenous supplementation of additives (i.e cofactors) making these strategies

more appealing alternatives for industrial processes. Herein, we encourage scientific community to develop more efficient biocatalysts but also processes with much higher capacity to recycle solvents and enzymes to make biocatalysis really sustainable.

ASSOCIATED CONTENT

Supporting Information.

Determination of Lagmuir isotherms, figures S1-S8 and table S1 (PDF). This material is available free of charge via the Internet at <http://pubs.acs.org>.

AUTHOR INFORMATION

Corresponding Authors

* E-mail (López-Gallego, F.): flopezgallego@unizar.es

* E-mail (Paradisi, F.): francesca.paradisi@nottingham.ac.uk

Author Contributions

The manuscript was written through contributions of all authors. All authors have given approval to the final version of the manuscript.

Notes

The authors declare no conflict of interest.

ACKNOWLEDGMENTS

We want to acknowledge ARAID foundation for funding F.L.G. and to MINECO (BIO2015-69887-R) for funding A.I.B.M and F.L.G. This work was also supported for M.L.C. and F.P. by BBSRC [grant number BB/P002536/1]. F.L.G. and F.P. thank the support of COST action CM1303-System biocatalysis that made possible this collaborative research funding A.I.B.M. short-stay at University of Nottingham. S.V.L. is grateful for the postdoctoral fellowship received from the Mexican Council for Science and Technology (CONACyT). The authors wish to thank Resindion S.R.L. and Purolite for kindly donating us different methacrylate porous resins.

ABBREVIATIONS

CLSM, Confocal laser scanning microscopy; Cv- ω TA, ω -transaminase from *Chromobacterium violaceum*; EC-Co²⁺, Sepabeads EC-EP/S beads activated with cobalt quelates; EC-Co²⁺/eA, Sepabeads EC-EP/S beads activated with both cobalt quelates and ethanolamine; EC-Co²⁺/PEI, Sepabeads EC-EP/S beads activated with cobalt quelates and coated with PEI; IDA, Iminodiacetic acid; He- ω TA, ω -transaminase from *Halomonas elongata*; K_d, dissociation constant; PBR, packed-bed reactors; PEI, Polyethyleneimine; Pf- ω TA, ω -transaminase from *Pseudomonas fluorescens*; PLP, Pyridoxal 5'-phosphate; Pu-Co²⁺, Purolite ECR8215F beads activated with cobalt quelates; Pu-Co²⁺/eA, Purolite ECR8215F beads activated with both cobalt quelates and ethanolamine; Pu-Co²⁺/hA, Purolite ECR8215F beads activated with both cobalt quelates and hydroxylamine; ω TAs, ω -transaminases.

REFERENCES

1. Constable, D. J. C.; Dunn, P. J.; Hayler, J. D.; Humphrey, G. R.; Leazer, J. J. L.; Linderman, R. J.; Lorenz, K.; Manley, J.; Pearlman, B. A.; Wells, A.; Zaks, A.; Zhang, T. Y. Key green chemistry research areas-a perspective from pharmaceutical manufacturers. *Green Chem.* **2007**, *9* (5), 411-420, DOI 10.1039/B703488C
2. Abrahamson, M. J.; Vazquez-Figueroa, E.; Woodall, N. B.; Moore, J. C.; Bommarius, A. S. Development of an amine dehydrogenase for synthesis of chiral amines. *Angew. Chem. Int. Ed.* **2012**, *51* (16), 3969-3972, DOI 10.1002/anie.201107813
3. Park, E. S.; Dong, J. Y.; Shin, J. S. omega-Transaminase-catalyzed asymmetric synthesis of unnatural amino acids using isopropylamine as an amino donor. *Org. Biomol. Chem.* **2013**, *11* (40), 6929-6933, DOI 10.1039/C3OB40495A
4. Yasukawa, K.; Nakano, S.; Asano, Y. Tailoring D-amino acid oxidase from the pig kidney to R-stereoselective amine oxidase and its use in the deracemization of alpha-methylbenzylamine. *Angew. Chem. Int. Ed.* **2014**, *53* (17), 4428-4431, DOI 10.1002/anie.201308812
5. Guo, F.; Berglund, P. Transaminase biocatalysis: optimization and application. *Green Chem.* **2017**, *19* (2), 333-360, DOI 10.1039/C6GC02328B
6. Kelly, S. A.; Pohle, S.; Wharry, S.; Mix, S.; Allen, C. C. R.; Moody, T. S.; Gilmore, B. F. Application of ω -Transaminases in the pharmaceutical industry. *Chem. Rev.* **2018**, *118* (1), 349-367, DOI 10.1021/acs.chemrev.7b00437
7. Slabu, I.; Galman, J. L.; Lloyd, R. C.; Turner, N. J. Discovery, Engineering, and synthetic application of transaminase biocatalysts. *ACS Catal.* **2017**, *7* (12), 8263-8284, DOI 10.1021/acscatal.7b02686

8. Weber, N.; Gorwa-Grauslund, M.; Carlquist, M. Exploiting cell metabolism for biocatalytic whole-cell transamination by recombinant *Saccharomyces cerevisiae*. *Appl. Microbiol. Biotechnol.* **2014**, *98* (10), 4615-4624, DOI 10.1007/s00253-014-5576-z
9. Kim, H. J.; Kim, Y. H.; Shin, J. H.; Bhatia, S. K.; Sathiyarayanan, G.; Seo, H. M.; Choi, K. Y.; Yang, Y. H.; Park, K. Optimization of direct lysine decarboxylase biotransformation for cadaverine production with whole-cell biocatalysts at high lysine concentration. *J. Microbiol. Biotechnol.* **2015**, *25* (7), 1108-1113, DOI 10.4014/jmb.1412.12052.
10. Neto, W.; Schürmann, M.; Panella, L.; Vogel, A.; Woodley, J. M. Immobilisation of ω -transaminase for industrial application: Screening and characterisation of commercial ready to use enzyme carriers. *J. Mol. Catal. B: Enzym.* **2015**, *117* 54-61, DOI 10.1016/j.molcatb.2015.04.005
11. Abaházi, E.; Sátorhelyi, P.; Erdélyi, B.; Vértessy, B. G.; Land, H.; Paizs, C.; Berglund, P.; Poppe, L. Covalently immobilized Trp60Cys mutant of ω -transaminase from *Chromobacterium violaceum* for kinetic resolution of racemic amines in batch and continuous-flow modes. *Biochem. Eng. J.* **2018**, *132* 270-278, DOI
12. Planchestainer, M.; Contente, M. L.; Cassidy, J.; Molinari, F.; Tamborini, L.; Paradisi, F. Continuous flow biocatalysis: production and in-line purification of amines by immobilised transaminase from *Halomonas elongata*. *Green Chem.* **2017**, *19* (2), 372-375, DOI 10.1016/j.bej.2018.01.022
13. Bajić, M.; Plazl, I.; Stloukal, R.; Žnidaršič-Plazl, P. Development of a miniaturized packed bed reactor with ω -transaminase immobilized in LentiKats®. *Process Biochem.* **2017**, *52* 63-72, DOI 10.1016/j.procbio.2016.09.021

14. Sheldon, R. A.; van Pelt, S. Enzyme immobilisation in biocatalysis: why, what and how. *Chem. Soc. Rev.* **2013**, *42* (15), 6223-6235, DOI 10.1039/c3cs60075k.
15. Cerioli, L.; Planchestainer, M.; Cassidy, J.; Tessaro, D.; Paradisi, F. Characterization of a novel amine transaminase from *Halomonas elongata*. *J. Mol. Catal. B: Enzym.* **2015**, *120* 141-150, DOI 10.1016/j.molcatb.2015.07.009
16. Andrade, L. H.; Kroutil, W.; Jamison, T. F. Continuous flow synthesis of chiral amines in organic solvents: immobilization of *E. coli* cells containing both ω -Transaminase and PLP. *Org. Lett.* **2014**, *16* (23), 6092-6095, DOI 10.1021/ol502712v
17. Velasco-Lozano, S.; Benítez-Mateos, A. I.; López-Gallego, F. Co-immobilized phosphorylated cofactors and enzymes as self-sufficient heterogeneous biocatalysts for chemical processes. *Angew. Chem. Int. Ed.* **2017**, *56* (3), 771-775, DOI 10.1002/anie.201609758
18. Benítez-Mateos, A. I.; San Sebastian, E.; Ríos-Lombardía, N.; Morís, F.; González-Sabín, J.; López-Gallego, F. Asymmetric reduction of prochiral ketones by using self-sufficient heterogeneous biocatalysts based on NADPH-dependent ketoreductases. *Chem. Eur. J.* **2017**, *23* (66), 16843-16852, DOI 10.1002/chem.201703475
19. Kaulmann, U.; Smithies, K.; Smith, M. E. B.; Hailes, H. C.; Ward, J. M. Substrate spectrum of ω -transaminase from *Chromobacterium violaceum* DSM30191 and its potential for biocatalysis. *Enzyme Microb. Technol.* **2007**, *41* (5), 628-637, DOI 10.1016/j.enzmictec.2007.05.011
20. Planchestainer, M.; Contente, M. L.; Cassidy, J.; Molinari, F.; Tamborini, L.; Paradisi, F. Continuous flow biocatalysis: production and in-line purification of amines by

- immobilised transaminase from *Halomonas elongata*. *Green Chem.* **2017**, *19*, 372-375, DOI 10.1039/C6GC01780K
21. Bradford, M. M. A rapid and sensitive method for the quantitation of microgram quantities of protein utilizing the principle of protein-dye binding. *Anal. Biochem.* **1976**, *72* (1), 248-254, DOI 10.1016/0003-2697(76)90527-3
 22. Holmes, K. L.; Lantz, L. M. Protein labeling with fluorescent probes. In *Methods in Cell Biology*. Darzynkiewicz, Z., Crissman, H. A., Robinson, J. P., Eds.; Elsevier Academic Press, 2001, DOI 10.1016/S0091-679X(01)63013-9
 23. Chen, S.; Berglund, P.; Humble, M. S. The effect of phosphate group binding cup coordination on the stability of the amine transaminase from *Chromobacterium violaceum*. *J. Mol. Catal.* **2018**, *446* 115-123, DOI 10.1016/j.mcat.2017.12.033
 24. Joshua, B.; P., D. R.; Sudipta, M.; L., R. C.; A., W. G. Ten-minute protein purification and surface tethering for continuous-flow biocatalysis. *Angew. Chem. Int. Ed.* **2017**, *56* (9), 2296-2301, DOI 10.1002/anie.201610821
 25. Van den Biggelaar, L.; Soumillion, P.; Debecker, D. P. Enantioselective transamination in continuous flow mode with transaminase immobilized in a macrocellular silica monolith. *Catalysts.* **2017**, *7* (2), 54, DOI 10.3390/catal7020054
 26. Chen, S. Stability and inactivation mechanisms of two transaminases. Ph.D. Dissertation, KTH Royal Institute of Technology, School of Engineering Sciences in Chemistry, Biotechnology and Health, Stockholm, 2018.

TABLE OF CONTENTS

The co-immobilization of ω -transaminase and PLP onto porous supports allows an efficient recycle of both enzyme and cofactor paving the way towards a more sustainable and cost-saving flow-biocatalysis.

